Applied Physics Letters

Magnetic field-controlled $0-\pi$ transitions and their experimental signatures in superconductor-ferromagnet-superconductor junctions

Cite as: Appl. Phys. Lett. **116**, 092601 (2020); https://doi.org/10.1063/1.5143269
Submitted: 23 December 2019 . Accepted: 14 February 2020 . Published Online: 02 March 2020

A. Vargunin, and M. A. Silaev

Applied Physics Letters ARTICLE scitation.org/journal/apl

Magnetic field-controlled 0−π transitions and their experimental signatures in superconductor-ferromagnet-superconductor junctions

Cite as: Appl. Phys. Lett. **116**, 092601 (2020); doi: 10.1063/1.5143269
Submitted: 23 December 2019 · Accepted: 14 February 2020 ·
Published Online: 2 March 2020

A. Vargunin[1,2] and M. A. Silaev[1,3,a)]

AFFILIATIONS

[1]Department of Physics and Nanoscience Center, University of Jyväskylä, P.O. Box 35 (YFL), Jyväskylä FI-40014, Finland
[2]Institute of Physics, University of Tartu, Tartu EE-50411, Estonia
[3]Moscow Institute of Physics and Technology, Dolgoprudny 141700, Russia

[a)]**Author to whom correspondence should be addressed:** mikesilaev@gmail.com

ABSTRACT

Superconductor-ferromagnet-superconductor Josephson junctions are known to exist in the 0 and π states with the transitions between them controlled by the temperature and ferromagnetic interlayer thickness. We demonstrate that these transitions can be controlled also by the external magnetic field directed perpendicular to the layers. By varying the ratio of diffusion coefficients in superconducting and ferromagnetic layers, these field-controlled transitions can be made detectable for arbitrary large values of the exchange energy in the ferromagnet. We also show that the $0-\pi$ transitions in the perpendicular field can be observed as the specific features of the flux-flow conductivity dependencies on the ferromagnetic thickness in accordance with recent experimental results.

Superconductor-ferromagnet-superconductor (SFS) junctions such as that shown schematically in Fig. 1 are known to have either a 0 or π ground state Josephson phase difference.[1,2] Switching between these states controlled by parameters such as temperature T and ferromagnetic interlayer thickness d_F is governed by the oscillations of Cooper pair wave functions as a result of the energy splitting between the spin-up and spin-down states introduced by the exchange field h.[3,4]

Transitions between the 0 and π-states have been observed experimentally as the strong oscillations of the critical current of a junction.[5–8] The π state can also be revealed in the closed electric loop with an integrated SFS junction by the appearance of spontaneous supercurrents.[9] Nowadays, the π-junction state of SFS attracts much attention due to applications in the flux-quantum logic based memory cells[10–13] and superconducting qubit implementations.[14,15]

Although the 0-π transition can be observed by changing the temperature for weak ferromagnets with small h,[5] this can be more challenging in systems with $h \gg T_{c0}$, where we denote T_{c0} to be the bulk critical temperature of the superconducting layer. This can be illustrated using the temperature-thickness phase diagram in Fig. 2(a) calculated at $B = 0$ as described below for the structure shown schematically in the upper left panel in Fig. 1. For large exchange fields, $h = 20T_{c0}$, the boundary between 0 and π states is almost vertical, so that one should control d_F with very high precision to spot the region of temperature-controlled transition. The origin of this behavior can be understood by considering the complex length $\xi_F^{-1} = \sqrt{(T + ih)/D_F}$, which determines the behavior of superconducting correlations in the F layer characterized by diffusion coefficient D_F. For $h \gg T_{c0}$, the scale is temperature-independent for the considered regime $T < T_{c0}$, and hence, the 0-π switching occurs at the same d_F for all temperatures. Thus, the only way to switch SFS regularly from the 0 to π state in this case is to scan over d_F, which requires fabrication and measuring many samples.

Here, we show that this situation can be improved by introducing the additional control parameter, which is the magnetic field B perpendicular to the layers. Unlike temperature-driven 0-π transition, which requires weak F and fine tuning of the F thickness, we show that the interval of F thicknesses suitable for field-driven transition can be made arbitrarily wide for any exchange field by reducing the diffusion constant of S with respect to the one in F.

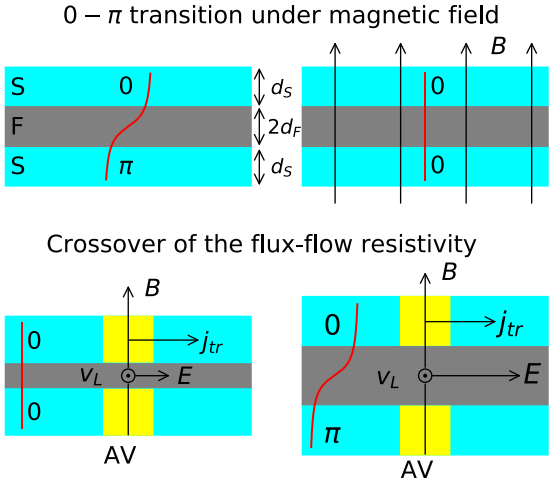

FIG. 1. Upper panels: perpendicular magnetic field $\boldsymbol{B}$ results in the transition from the π to the 0-state. Lower panel: Crossover of the flux-flow resistivity ρ_{ff} upon the 0-π transition with the change in F thickness. v_L is the velocity of Abrikosov vortex (AV, yellow), $\boldsymbol{j}_{tr}$ is the transport current, and $\boldsymbol{E} = \rho_{ff}\boldsymbol{j}_{tr}$ is the electric field.

In the case of the applied perpendicular magnetic field, the scale of oscillations in the F layer is determined at small temperatures $T \ll q$ by $\xi_F^{-1}(B) = \sqrt{(q+ih)/D_F}$, where $q = eBD_F$. Then, even for arbitrary large h, the orbital effect can introduce a significant shift of ξ_F if $q \sim h$. This condition can be achieved if the orbital depairing can be made sufficiently strong. The largest values of q can be obtained near the upper critical field $B = H_{c2}$. By taking into account estimation $eH_{c2}D_S \sim 1$, the regime $q \sim h$ requires the diffusion coefficient in the superconductor D_S much smaller than that in the ferromagnet $D_S \ll D_F$. This condition can be always achieved by intentionally adding impurities and decreasing electron scattering time in dirty S. The effect is demonstrated in Figs. 2(b) and 2(c) as a significant shift of the F thickness segregating 0 and π states from its zero-field value by applying a magnetic field.

In the intermediate region of perpendicular magnetic fields $0 < B < H_{c2}$, the SFS junction is in the mixed state, which means that it is pierced by the Abrikosov vortex lines. The natural question is how the 0 and π superconducting states manifest themselves in the vortex behavior. In principle, the discrepancy between distributions of the gap order parameter in these states results in different responses to the applied magnetic field. This was revealed recently, for instance, by superfluid-density measurements.[16]

The characteristic feature of the mixed state is a non-zero resistivity, which occurs due to the dissipative motion of mobile vortex lines in the superconducting environment. Below we show that distinct gap profiles of the 0 and π-states lead also to the difference in the flux-flow resistivity of SFS. We demonstrate that one can detect 0-π transitions measuring the qualitative change in the dependence of resistivity on d_F in the perpendicular magnetic field.

Below we present a theoretical description consistent with available flux-flow resistivity data for SFS[17] and discuss a low-field flux-flow resistivity experiment, where the resistivity of SFS is proportional to the vortex density in agreement with Bardeen-Stephen theory. We argue that in the π-state, the relevant numeric proportionality coefficient exhibits universal h-independent behavior, providing a way to distinguish between the 0 and π states of SFS by single flux-flow resistivity measurement.

Model. We start with the formalism of quasiclassical Green's function (GF)[18] generalized to describe non-equilibrium spin states in diffusive superconductors,[19] $\check{g}(t_1,t_2,\mathbf{r}) = \begin{pmatrix} \hat{g}^R & \hat{g}^K \\ 0 & \hat{g}^A \end{pmatrix}$, where $\hat{g}^{R/A/K}$ are the retarded/advanced/Keldysh components, which are determined by the Keldysh-Usadel equation

$$\{\hat{\tau}_3\partial_t, \check{g}\}_t = \hat{\partial}_{\boldsymbol{r}}\hat{D}(\check{g}\circ\hat{\partial}_{\boldsymbol{r}}\check{g}) - i\left[\hat{\tau}_3\hat{H}, \check{g}\right]_t, \tag{1}$$

where $\hat{D}$ is the diffusivity tensor, which can be anisotropic and space-dependent, $\hat{H} = \hat{\boldsymbol{\sigma}}\boldsymbol{h} - \hat{\tau}_1\hat{\Delta}$, $\hat{\tau}_i$ and $\hat{\sigma}_i$ $(i = 0,1,2,3)$ are Pauli matrices in Nambu and spin space, and $\boldsymbol{h}$ is the exchange field. The gap function $\hat{\Delta} = |\Delta|e^{-i\hat{\tau}_3\varphi}$, where φ is the gap phase, is determined by the self-consistency condition

$$\Delta = \pi\lambda \mathrm{Tr}\hat{g}^K_{12}(t,t)/4, \tag{2}$$

where λ is the coupling constant finite in S layers. In Eq. (1), the commutator operator is defined as $[X,g]_t = X(t_1)g(t_1,t_2) - g(t_1,t_2)X(t_2)$, similarly for anticommutator $\{,\}_t$. The symbolic product operator is given by $(A\circ B)(t_1,t_2) = \int dt A(t_1,t)B(t,t_2)$, and the covariant differential superoperator reads as $\hat{\partial}_{\boldsymbol{r}} = \partial_{\boldsymbol{r}} - ie\boldsymbol{A}[\hat{\tau}_3,\cdot]$, where e is the

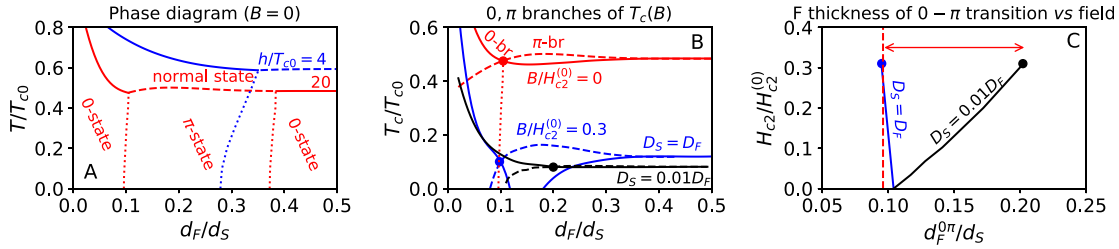

FIG. 2. (a) Zero-field $B = 0$ phase diagram for the ground states of SFS for $h/T_{c0} = 20$ (red) and 4 (blue). The boundary between 0 (π) and the normal state is shown by solid (dashed), while 0-π transition is shown by dotted curves. In panel a, $D_S = D_F$. (b) Field-dependent critical temperatures of the transitions to 0 (solid) and π (dashed) states and their cross point (dots). Red: $B/H_{c2}^{(0)} = 0$. Blue and black: 0.3 for $D_S/D_F = 1$ and 0.01, respectively. $H_{c2}^{(0)}$ is the bulk upper critical field. The dotted line is the 0-π transition for $B = 0$. (c) Field dependencies of the 0-π transition thickness $d_F^{0\pi}$ determined by the cross points of the 0 and π branches of $T_c(B)$ for different D_S/D_F ratios. Each point on the curves has the temperature $T_c(B = H_{c2}, d_F^{0\pi})$. Dots correspond to $T_c(B = H_{c2}, d_F^{0\pi}) \to 0$. The dashed marker is $d_F^{0\pi}(B = 0, T = 0)$. The interval of the field-controlled 0-π transition occurring at $T \to 0$ is shown by the red arrow. In (b) and (c), $h/T_{c0} = 20$, and in all panels, $d_S = 3.3\xi$, where $2\pi T_{c0}\xi^2 = D_F$.

elementary charge. The diffusion coefficient is different in S and F regions. For simplicity, we assume that F is isotropic $D_z = D_{x,y} = D_F$, while S is anisotropic with $D_z = D_F$ and $D_{x,y} = D_S$. The anisotropy assumption does not affect results qualitatively since they rely on the difference of diffusion coefficients in the direction perpendicular to the magnetic field, that is, along the layers.

First, we start with the equilibrium problem of the magnetic-field driven 0-π transitions. Our goal is to find the range of parameters where the system undergoes this transition with the changing magnetic field from 0 to H_{c2} in the direction perpendicular to SF interface, $\boldsymbol{B} = B\boldsymbol{z}$. To determine such parameters, it is enough to compare the states at the end points of this interval, namely, at $B = 0$ and at $B = H_{c2}$. We assume $\boldsymbol{h} = h\boldsymbol{z}$ in the F layer, put $\hat{g}(t_1, t_2) = \int_{-\infty}^{\infty} \hat{g}(\varepsilon, t) e^{-i\varepsilon(t_1 - t_2)} \frac{d\varepsilon}{2\pi}$, where $t = (t_1 + t_2)/2$, and use gradient expansion for time-convolution products to obtain equations for the temperature GF by replacing $-i\varepsilon$ with Matsubara frequency ω_n.

In the absence of magnetic field $B = 0$, we determined the lowest-energy state of the SFS system on the T-d_F plane by evaluating the free energy[20] using the self-consistent distribution of $\Delta(z)$ and corresponding GF. By comparing the numerical values of the 0 and π branches of free energy, we obtained the first-order 0-π transition lines shown in Fig. 2(a). Previously, thermodynamic 0-π transition was discussed only within Ginzburg–Landau theory.[21]

One can see that for parameters $h \gg T_{c0}$ typical for strong ferromagnets such as Co, the 0-π transition curve is almost vertical, that is, the threshold thickness $d_F^{0\pi}$ depends on the temperature very weakly. Practically, this means that it quite difficult to choose d_F in the range where the SFS system has temperature-controlled 0-π transition.

To find how the magnetic field changes critical temperatures of the 0 and π-states, we generalize the multi-mode approach used previously for SF bilayers.[22–24] Using the symmetry of solutions, we reduce the SFS problem to that of the SF bilayer with different boundary conditions at the free F interface corresponding to 0 and π states. We consider gauge $\boldsymbol{A} = \boldsymbol{y}Bx$ and apply the Abrikosov ansatz

$$\Delta = \sum_m C_m e^{impy} \tilde{\Delta}(x - mx_0, z), \tag{3}$$

$$\hat{g}_{12n} = \sum_{m,\sigma} C_m e^{impy} f_{\sigma n}(x - mx_0, z)\hat{\sigma}_\sigma. \tag{4}$$

Here, anomalous Matsubara GF (4) is extended into spin space by introducing $2\hat{\sigma}_\sigma = \hat{\sigma}_0 + \sigma\hat{\sigma}_3$, where $\sigma = \pm$. Other notations are conventional for lattice solution, namely, $|C_m| = 1$, p is defined by lattice symmetry, $x_0 = pL_H^2$, and $L_H^{-2} = 2eB$. Next, we separate variables $f_{\sigma n}(x, z) = \Psi_0(x)\alpha_{\sigma n}(z)$ and $\tilde{\Delta}(x, z) = \Psi_0(x)\beta(z)$, where $\Psi_0 = e^{-L_H^{-2}x^2/2}$ is zero Landau level eigenfunction, to obtain the Usadel equation in the form

$$D_z\partial_z^2\alpha_{\sigma n} - 2[(\omega_n + q + i\sigma h)\alpha_{\sigma n} + i\beta] = 0, \tag{5}$$

together with self-consistency condition $\beta = \lambda\pi iT\sum_{\sigma, n\geq 0}\alpha_{\sigma n}$. Here, $q = eBD_x$ is the orbital energy. We solve Eq. (5) together with boundary conditions and the self-consistency equation by means of the multi-mode approach, yielding the upper critical field $H_{c2} = H_{c2}(T)$ or field-dependent critical temperature $T_c = T_c(B)$.

The resulting dependencies $T_c = T_c(d_F)$ for different B values are shown in Fig. 2(b). For small magnetic fields, we have intersecting 0 and π branches, resulting in the oscillatory behavior of $T_c(d_F)$.[22,25,26]

For larger B, there appear intervals of d_F with only one stable state, either 0 or π as shown by blue curves in Fig. 2(b). The 0-π transitions occur at the values of thickness $d_F^{0\pi}$ determined by the intersection of 0 and π branches of $T_c(d_F)$ [shown by dots in Fig. 2(b)]. Figure 2(c) demonstrates the magnetic field dependence of $d_F^{0\pi}$, confirming our qualitative arguments about its high sensitivity to the ratio of diffusion coefficients in F and S layers. For $D_F/D_S > h/T_{c0}$ [black line in Fig. 2(c)], there is a strong variation of threshold thickness with the field as compared with almost no dependence of $d_F^{0\pi}$ in the opposite case [blue line in Fig. 2(c)].

To understand the SFS behavior under the applied magnetic field, it is enough to compare the endpoints, which are the states at $B = 0$ and at $B = H_{c2}$ shown in Figs. 2(a) and 2(c), respectively. In Fig. 2(c), the 0 states at $B = H_{c2}$ are on the left of the corresponding solid curve, while π states at $B = 0$ and $T = 0$ are on the right of the dashed line. For larger T, the shift of the dashed line is negligible as can be inferred from Fig. 2(a). From the comparison of dashed and solid black lines in Fig. 2(c), one can see that for $D_S = 0.01D_F$, there is a wide interval of d_F, where the 0-π transition *with necessity* occurs when varying the magnetic field from 0 to H_{c2} at fixed T and d_F. This interval bounded by the $d_F^{0\pi}(H_{c2})$ curve and $d_F^{0\pi}(B = 0)$ value is shown by the red arrow in Fig. 2(c).

Flux-flow resistivity. At intermediate values of the magnetic field $0 < B < H_{c2}$, the SFS system is in the mixed state consisting of Abrikosov vortex (AV) lines shown schematically in lower panels of Fig. 1. The vortex structure transforms due to the proximity effect.[27,28] Such a transformation is different in the 0 and π states of the SFS system, which affects their dynamical properties as shown below.

To calculate the structure of individual vortices at finite magnetic fields, we use the circular cell approximation,[29–32] where the unit cell of the hexagonal vortex lattice hosting a single vortex is replaced by a circular cell with the center at the point of the superconducting phase singularity. Inside the circular cell, the gap and magnetic field distributions are taken radially symmetric with respect to the cell center. At this, the circular-cell radius is uniquely defined by magnetic induction, $r_c = \sqrt{\phi_0/(\pi B)}$, so that there is exactly one flux quantum $\phi_0 = \pi/e$ passing through the unit vortex cell. The calculated gap profile inside the cell is shown in Fig. 3.

The controlled motion of the vortices can be produced by applying transport current $\boldsymbol{j}_{tr}$, which exerts the Lorentz force $\boldsymbol{F}_L = \phi_0\boldsymbol{j}_{tr} \times \boldsymbol{z}$ on each vortex due to the interaction with its local magnetic field. Vortex motion with velocity $\boldsymbol{v}_L$ produces perpendicular electric field $\boldsymbol{E} = \boldsymbol{B} \times \boldsymbol{v}_L$ as shown in Fig. 1. This field causes energy dissipation due to the Ohmic losses inside the normal vortex core, which can be

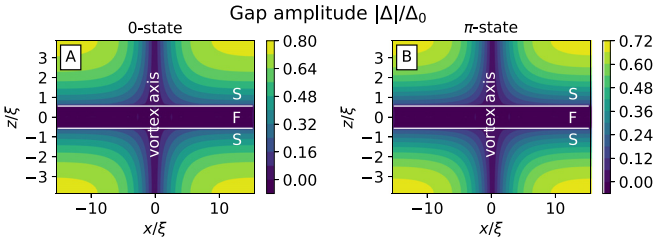

FIG. 3. Normalized gap in the vortex cell of SFS for the 0 (a) and π-states (b). Here, $d_F/d_S = 0.17$, $h/T_{c0} = 6$, and $D_S = D_F$. White horizontal lines are SF interfaces.

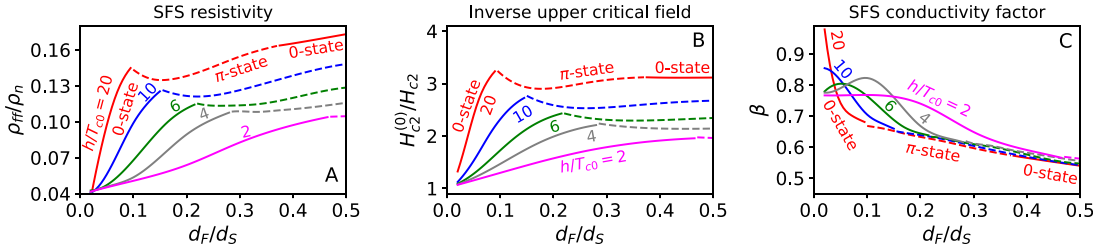

FIG. 4. (a) The crossover of ρ_{ff} at the 0-π transition. (b) Inverse upper critical field $H_{c2}^{-1}(d_F)$. (c) The numerical factor β in Bardeen–Stephen expression. In (a)–(c), $T = 0.055T_{c0} \ll T_c$, $D_S = D_F$, and colors indicate different $h/T_{c0} = 2, 4, 6, 10, 20$. Solid and dashed curves are stable 0 and π branches. In (a) and (c), $B = 0.03H_{c2}^{(0)} \ll H_{c2}$.

expressed as the viscous friction $\boldsymbol{F} = -\eta \boldsymbol{v}_L$, where η is the vortex viscosity. In the steady-state regime, $\boldsymbol{F} + \boldsymbol{F}_L = 0$, we obtain $\boldsymbol{E} = \rho_{ff}\boldsymbol{j}_{tr}$, where $\rho_{ff} = \phi_0 B/\eta$ is the flux-flow resistivity.

To calculate viscosity η, we consider microscopic expression[33,34] for the force $\boldsymbol{F}$ acting due to the non-equilibrium environment. The latter is determined by the vortex-motion induced deviations of the electron distribution function from the Fermi–Dirac one, which obeys kinetic equations derived from the Keldysh part of the Keldysh-Usadel equation (1). The coefficients in kinetic equations are determined by the vortex structure that we find from the equilibrium problem as explained above. We consider the low-temperature regime where the nonequilibrium states have subgap energies and therefore their contributions relax at the distances of the order of coherence length. This is different from the vicinity of T_c, where vortex motion in multilayered systems is determined by the renormalization of long-range charge imbalance mode.[35]

In Fig. 4(b), we show the calculated ρ_{ff} for stable parts of the 0 and π branches. The intersection of these branches points to the first-order 0-π transition whose position scales with $\xi_F \sim 1/\sqrt{h}$. The crossover behavior of ρ_{ff} at 0-π transition can be understood qualitatively using the Bardeen–Stephen expression $\rho_{ff}/\rho_n = \beta^{-1}B/H_{c2}$, where $\beta \sim 1$ is determined by the particular microscopic model and ρ_n is the normal-state resistivity. The inverse upper critical field of the SFS trilayer[23,36] $H_{c2}^{-1}(d_F)$ is shown in Fig. 4(b). The variations of $H_{c2}^{-1}(d_F)$ follow closely the behavior of ρ_{ff}. Their oscillation in the vicinity of the 0-π transition is caused by the superconductivity suppression with d_F in the 0 and its enhancement in the π state. In the considered low-temperature regime, $\beta \approx 0.77$ for usual single-band dirty superconductors.[37] Figure 4(c) demonstrates dependencies $\beta(d_F)$ for SFS sandwich. We see that the bulk value is approached in the limit $d_F \to 0$, that is, in the absence of the F layer. For finite d_F, the function $\beta(d_F)$ passes in the 0-state through the maximum, whose height exceeds the bulk value of 0.77 for not very weak F. However, in the π-state, $\beta < 0.77$ approaches universal h-independent asymptotic weakly varying with d_F. These signatures of β can be used for distinguishing the state of SFS with the help of the single flux-flow resistivity experiment without fabricating and measuring many samples.

The results shown in Fig. 4(a) are in qualitative agreement with measurements demonstrating the increase followed by the saturation of flux-flow resistivity in the SFS trilayer with the growth of d_F.[17] Although oscillations of $\rho_{ff}(d_F)$ and the 0-π transition point were not directly detected in this experiment, even in such a case, flux-flow resistivity measurements allow us to distinguish between samples in the 0 and π states by means of the β value, as discussed above.

To conclude, we have demonstrated the possibility of the 0-π transitions in the SFS structure driven by the perpendicular magnetic field. These transitions can be achieved in the wide interval of the F layer thicknesses provided that the S layer has a much smaller diffusion coefficient than the F layer. In contrast to the temperature-driven ones, the magnetic field-driven 0-π transitions can be realized in principle for arbitrary large exchange field $h \gg T_c$. Besides this, we have found indications of 0-π transitions in the flux-flow conductivity of the SFS structure. This behavior is in qualitative agreement with experimental observations.

See the supplementary material for theoretical details.

This work was supported by the Academy of Finland (Project No. 297439), the Russian Science Foundation (Grant No. 19-19-00594), and the European Regional Development Fund (Mobilitas Pluss under Grant No. MOBTP152). It is our pleasure to acknowledge discussions with M. Yu. Kupriyanov, M. M. Khapaev, N. Pompeo, and A. S. Mel'nikov.

REFERENCES

[1] A. I. Buzdin, L. Bulaevskii, and S. Panyukov, JETP. Lett. **35**, 178 (1982).
[2] A. I. Buzdin and M. Y. Kupriyanov, JETP. Lett. **53**, 321 (1991).
[3] A. I. Buzdin, Rev. Mod. Phys. **77**, 935 (2005).
[4] I. F. Lyuksyutov and V. L. Pokrovsky, Adv. Phys. **54**, 67 (2005).
[5] V. V. Ryazanov, V. A. Oboznov, A. Y. Rusanov, A. V. Veretennikov, A. A. Golubov, and J. Aarts, Phys. Rev. Lett. **86**, 2427 (2001).
[6] T. Kontos, M. Aprili, J. Lesueur, F. Gent, B. Stephanidis, and R. Boursier, Phys. Rev. Lett. **89**, 137007 (2002).
[7] V. Shelukhin, A. Tsukernik, M. Karpovski, Y. Blum, K. Efetov, A. Volkov, T. Champel, M. Eschrig, T. Löfwander, G. Schoen *et al.*, "Observation of periodic π-phase shifts in ferromagnet-superconductor multilayers," Phys. Rev. B **73**, 174506 (2006).
[8] V. A. Oboznov, V. V. Bolginov, A. K. Feofanov, V. V. Ryazanov, and A. I. Buzdin, Phys. Rev. Lett. **96**, 197003 (2006).
[9] A. Bauer, J. Bentner, M. Aprili, M. L. D. Rocca, M. Reinwald, W. Wegscheider, and C. Strunk, Phys. Rev. Lett. **92**, 217001 (2004).
[10] E. Terzioglu and M. R. Beasley, IEEE Trans. Appl. Supercond. **8**, 48 (1998).
[11] A. V. Ustinov and V. K. Kaplunenko, J. Appl. Phys. **94**, 5405 (2003).
[12] M. I. Khabipov, D. V. Balashov, F. Maibaum, A. B. Zorin, V. A. Oboznov, V. V. Bolginov, A. N. Rossolenko, and V. V. Ryazanov, Supercond. Sci. Technol. **23**, 045032 (2010).
[13] S. Bakurskiy, N. Klenov, I. Soloviev, N. Pugach, M. Y. Kupriyanov, and A. Golubov, "Protected 0-π states in sisfs junctions for josephson memory and logic," Appl. Phys. Lett. **113**, 082602 (2018).
[14] T. Yamashita, K. Tanikawa, S. Takahashi, and S. Maekawa, Phys. Rev. Lett. **95**, 097001 (2005).

[15]A. K. Feofanov, V. A. Oboznov, V. V. Bol'ginov, J. Lisenfeld, S. Poletto, V. V. Ryazanov, A. N. Rossolenko, M. Khabipov, D. Balashov, A. B. Zorin, P. N. Dmitriev, V. P. Koshelets, and A. V. Ustinov, Nat. Phys. **6**, 593 (2010).
[16]M. J. Hinton, S. Steers, B. Peters, F. Y. Yang, and T. R. Lemberger, Phys. Rev. B **94**, 014518 (2016).
[17]K. Torokhtii, N. Pompeo, C. Meneghini, C. Attanasio, C. Cirillo, E. A. I. amd, S. Sarti, and E. Silva, J. Supercond. Novel Magn. **26**, 571 (2013).
[18]A. Schmid and G. Schön, J. Low Temp. Phys. **20**, 207 (1975).
[19]F. S. Bergeret, M. Silaev, P. Virtanen, and T. T. Heikkilä, Rev. Mod. Phys. **90**, 041001 (2018).
[20]P. Virtanen, A. Vargunin, and M. Silaev, "Quasiclassical expressions for the free energy of superconducting systems," arXiv:1909.00992 (2019).
[21]A. V. Samokhvalov and A. I. Buzdin, Phys. Rev. B **92**, 054511 (2015).
[22]Y. V. Fominov, N. M. Chtchelkatchev, and A. A. Golubov, Phys. Rev. B **66**, 014507 (2002).
[23]B. Krunavakarn and S. Yoksan, Physica C **440**, 25 (2006).
[24]T. Karabassov, V. S. Stolyarov, A. A. Golubov, V. M. Silkin, V. M. Bayazitov, B. G. Lvov, and A. S. Vasenko, Phys. Rev. B **100**, 104502 (2019).
[25]J. Jiang, D. Davidovic, D. H. Reich, and C. L. Chien, Phys. Rev. Lett. **74**, 314 (1995).
[26]A. V. Samokhvalov, Phys. Solid State **59**, 2143 (2017).
[27]A. A. Golubov, M. Y. Kupriyanov, and M. M. Khapaev, "Abrikosov vortices in sf bilayers," JETP Lett. **104**, 847–851 (2016).
[28]V. S. Stolyarov, T. Cren, C. Brun, I. A. Golovchanskiy, O. V. Skryabina, D. I. Kasatonov, M. M. Khapaev, M. Y. Kupriyanov, A. A. Golubov, and D. Roditchev, "Expansion of a superconducting vortex core into a diffusive metal," Nat. Commun. **9**, 2277 (2018).
[29]D. Ihle, Phys. Status Solidi B **47**, 429 (1971).
[30]R. J. Watts-Tobin, L. Kramer, and W. Pesch, J. Low Temp. Phys. **17**, 71 (1974).
[31]J. Rammer, W. Pesch, and L. Kramer, Z. Phys. B **68**, 49 (1987).
[32]J. Rammer, J. Low Temp. Phys. **71**, 323 (1988).
[33]A. I. Larkin and Y. N. Ovchinnikov, *Modern Problems in Condensed Matter Sciences: Nonequilibrium Superconductivity*, edited by D. N. Langenberg and A. I. Larkin (Elsevier, 1986), p. 493.
[34]N. B. Kopnin, *Theory of Nonequilibrium Superconductivity* (Oxford University Press, 2001).
[35]A. S. Mel'nikov, "Inertial mass and viscosity of tilted vortex lines in layered superconductors," Phys. Rev. Lett. **77**, 2786 (1996).
[36]Z. Radović, M. Ledvij, and L. Dobrosavljević-Grujić, Solid State Commun. **80**, 43 (1991).
[37]A. Vargunin and M. A. Silaev, Phys. Rev. B **96**, 214507 (2017).